catalysts

MDPI

Article

Photocatalytic Degradation of Azo Dye Reactive Violet 5 on Fe-Doped Titania Catalysts under Visible Light Irradiation

Antonio Zuorro [1,*], Roberto Lavecchia [1], Marika Michela Monaco [1], Giuseppina Iervolino [2] and Vincenzo Vaiano [2]

[1] Department of Chemical Engineering, Materials and Environment, Sapienza University, 00184 Rome, Italy
[2] Department of Industrial Engineering, University of Salerno, 84084 Fisciano (SA), Italy
* Correspondence: antonio.zuorro@uniroma1.it; Tel.: +390644585598

Received: 21 June 2019; Accepted: 26 July 2019; Published: 29 July 2019

Abstract: The presence of azo dyes in textile effluents is an issue of major concern due to their potential impact on the environment and human health. In this study we investigate the photocatalytic degradation under visible light of Reactive Violet 5 (RV5), an azo dye widely used in the textile industry. A preliminary screening of different titania-based catalysts was carried out to identify the best candidate for RV5 removal. The selected catalyst was then tested in a stirred and aerated lab-scale reactor illuminated with a blue light-emitting diode (LED) source emitting in the wavelength range of 460–470 nm. The effects of pH, catalyst load, and hydrogen peroxide additions on the efficiency of dye removal were evaluated. Under the best conditions (pH 10, 3 g/L of catalyst, and 60 mM hydrogen peroxide), the dye solution was completely decolorized in about 2 h. Overall, the results obtained suggest that the proposed process may represent a suitable method for the removal of RV5 from textile effluents.

Keywords: photocatalysis; visible light; titania catalysts; azo dye; reactive violet 5; textile wastewater

1. Introduction

Azo dyes are the largest class of dyes used in industry [1]. These compounds are characterized by the presence of one or more azo bonds (–N=N–) in their molecule in association with one or more aromatic structures [2]. In the textile industry, the use of azo dyes for coloring cellulosic fibers such as cotton and wool has increased significantly over the last few decades due to their cost effectiveness, brightness of color, and good resistance to washing and light exposure. A major drawback related to their application on textiles is the low fixation yield of the dye on the fiber caused by the hydrolysis of the reactive groups in the dye molecule [3]. As a result, up to about 30% of the initial amount of dye can be lost in water [4].

The presence of azo dyes in textile effluents makes them particularly harmful to the environment and to human health [5]. In fact, their release into aquatic ecosystems may lead to a reduction of sunlight penetration and dissolved oxygen concentration, with deleterious effects on local flora and fauna [6]. In addition, toxic and potentially carcinogenic compounds such as aromatic amines can be formed during dye degradation [7]. For these reasons, textile wastewater needs to be properly treated.

Since conventional water treatments are often ineffective in eliminating azo dyes from textile effluents, more efficient technologies, such as advanced oxidation processes (AOPs), are used [8,9]. AOPs are based on the generation of highly reactive radical species, such as hydroxyl radicals ($^{\bullet}$OH), by solar, chemical, or other forms of energy. These radicals can attack the target compounds through different reaction mechanisms, leading to their degradation [10,11].

Among the AOPs, heterogeneous photocatalysis is a very promising technology for the removal of water pollutants [12,13]. One of the most studied photocatalysts is represented by TiO_2, due to its high stability, chemical inertness, non-toxicity, and low cost [14]. TiO_2 is characterized by a band gap energy value of 3.2 eV, which corresponds to a prevalent photocatalyst activation under UV light [15]. Moreover, when the TiO_2 semiconductor is activated by UV light, an extremely reactive electron–hole pair is created. However, this reactive pair can easily recombine. In order to delay this recombination, different approaches have been investigated, such as catalyst doping or surface modifications by the addition of various anionic and cationic elements [16]. The introduction of doping elements in the catalyst structure can result in the successful reduction of activating light frequencies from UV to the visible region. This is a very positive aspect as it allows the use of solar light to activate the photocatalyst [17]. Noble metals such as Pt, Pd, or Au can be effectively used as doping elements [18,19]. When present in the crystalline structure of the catalyst, they inhibit the recombination of electron charges and allow its activation under visible light [20,21]. Unfortunately, these metals are expensive, which has prompted the search for alternative and cheaper doping elements, such as Fe and Cu ions [22,23]. In particular, the use of a Fe-doped TiO_2 photocatalyst for the degradation of methyl orange [24] and methylene blue [25] dyes and for the oxidation of arsenite [26] has been reported, underlining the interest of the scientific community for the application of this kind of semiconductor.

In this paper we investigate the degradation of Reactive Violet 5 (RV5) by a photocatalytic treatment with Fe-doped TiO_2 photocatalysts exposed to visible light. RV5 is widely used in textile dyeing because of its brightness, ease of application, and good fastness to washing. However, its complex aromatic structure (Figure 1) makes it highly resistant to degradation. A literature survey showed that very few studies have been performed on RV5 degradation and none of them investigated the photocatalytic removal of the dye under visible light [27–32]. Accordingly, a first aim of this study was to evaluate whether the use of the selected photocatalyst in the presence of visible light could be a suitable method to degrade RV5. Second, we were interested in assessing the effect of the main process parameters on the efficiency of dye removal and the possibility of enhancing it through the addition of hydrogen peroxide.

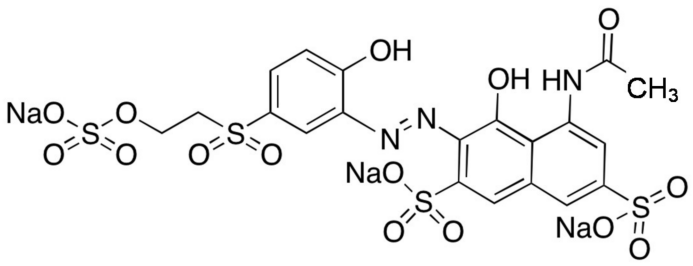

Figure 1. Chemical structure of azo dye Reactive Violet 5 (RV5).

The results obtained indicated that the proposed process may represent a viable and promising approach for the removal of RV5 from textile effluents.

2. Results and Discussion

2.1. Catalyst Characterization

The XRD results of undoped and doped TiO_2 with different Fe contents are reported in Figure 2. It was possible to observe that the crystalline structure of the photocatalysts showed only patterns related to anatase TiO_2 for all the samples [33]. No signals due to iron oxides appear in the XRD patterns, suggesting insignificant iron segregation in Fe-doped TiO_2 samples [34].

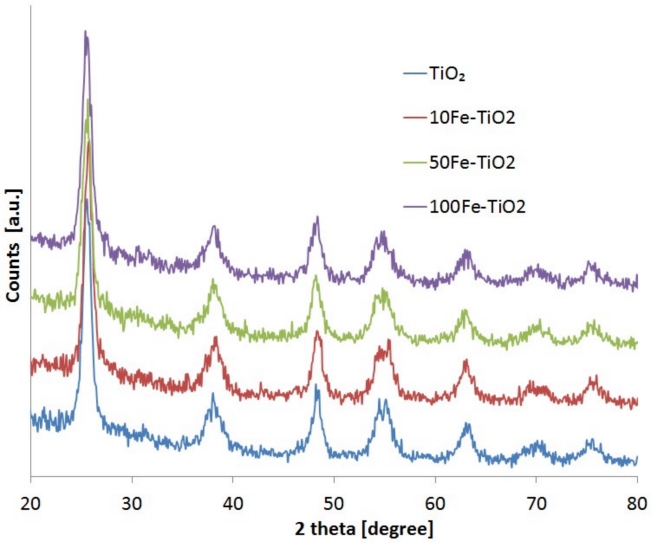

Figure 2. XRD spectra of the photocatalysts.

Since the ionic radius of the Fe^{3+} ion (0.064 nm) is smaller than that one of the Ti^{4+} ion (0.068 nm) [35], and considering that the Pauling electronegativities of Fe^{3+} (1.83) and Ti^{4+} (1.54) are similar [36], Fe^{3+} ions may enter the crystal cell of TiO_2 at substitutional sites [37]. To better investigate this aspect, the XRD spectra of the photocatalysts were more accurately analyzed in the range 20°–30° (Figure 3).

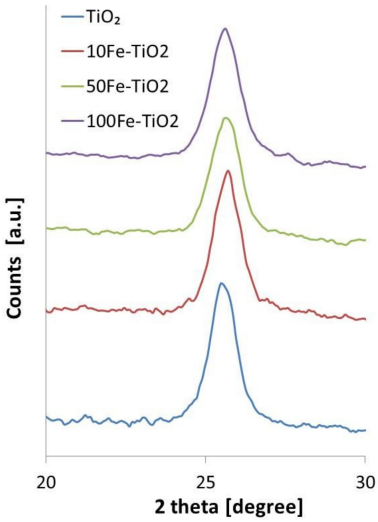

Figure 3. XRD spectra of the photocatalysts in the range 20°–30°.

It is possible to observe that the diffraction peak of undoped TiO_2 at about 25.3° shifted to a higher angle for all the Fe-doped TiO_2 samples, indicating that doping of TiO_2 with iron led to a decrease of the lattice parameters. This phenomenon was a clear indication that our preparation method for the doped photocatalysts induced a replacement of the lattice Ti^{4+} ions by Fe^{3+} ions [37], therefore evidencing the successful doping of the TiO_2 crystalline structure with iron.

The crystalline size of the photocatalysts was calculated on the diffraction pattern visualized in Figure 3 using Scherrer's formula (Table 1).

Table 1. List of the prepared photocatalyst and their characteristics.

Photocatalysts	Crystalline Size [nm]	Specific Surface Area [m^2/g]	Band Gap Energy [eV]
TiO_2	8.4	169	3.20
10Fe-TiO_2	8.3	171	3.12
50Fe-TiO_2	7.9	179	2.90
100Fe-TiO_2	7.9	179	2.63

The calculated crystalline size for undoped TiO_2 was 8.4 nm and only a slight decrease for Fe doped TiO_2 samples was observed. This phenomenon is possibly due to the entrance of Fe^{3+} into the TiO_2 lattice [38], inducing also an increase in the specific surface area values (Table 1) with respect to undoped TiO_2, as observed in the literature [39].

Raman spectra in the range of 200–800 cm^{-1} of the doped catalysts and undoped TiO_2 are shown in Figure 4. In particular, only the TiO_2 common signals at 144, 396, 514, and 637 cm^{-1} and a weak shoulder at 195 cm^{-1} due to the anatase crystalline phase of TiO_2 were evident [40]. Also in this case, no signals due to iron oxides were evident. These results confirmed that the TiO_2 doping process was correctly finalized.

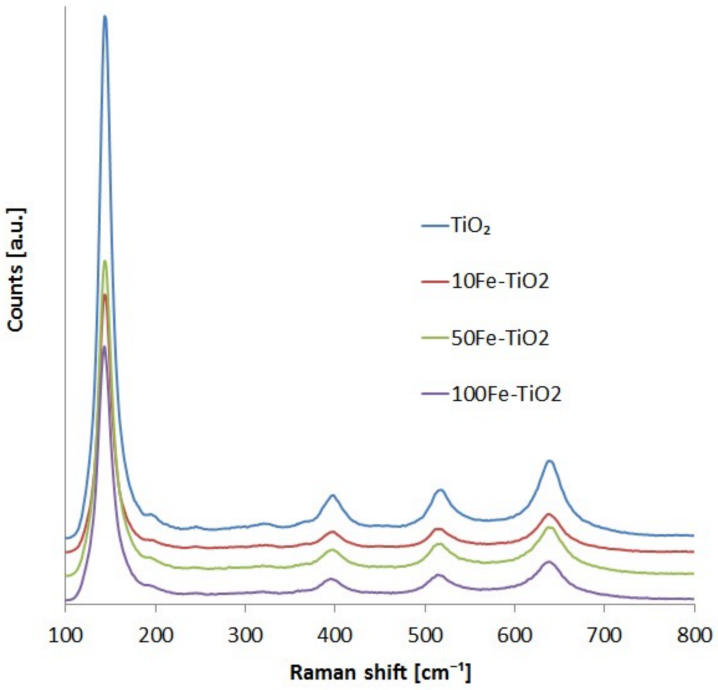

Figure 4. Raman spectra of undoped and Fe-doped TiO_2 photocatalysts in the range of 100–800 cm^{-1}.

Additionally, the intensity of the Raman bands for all the doped samples was lower than those of the undoped TiO_2, supporting again the incorporation of Fe^{3+} into the substitution site of the TiO_2 lattice [41].

The data obtained from UV–Vis reflectance spectra were used to evaluate the band-gap energy of TiO_2 and Fe-doped TiO_2 photocatalysts (Figure 5). The doping of TiO_2 with iron significantly influenced the band-gap energy value. In fact, as the Fe amount increased, a decrease in band-gap energy (from 3.20 for undoped TiO_2 to 2.63 eV for 100Fe-TiO_2) was observed. This decrease was likely due to the electronic transition from donor levels formed with dopants to the conduction band of the host photocatalyst [42]. The band-gap energy value of Fe-doped TiO_2 samples provided an indication of their potential photoactivity under visible light irradiation.

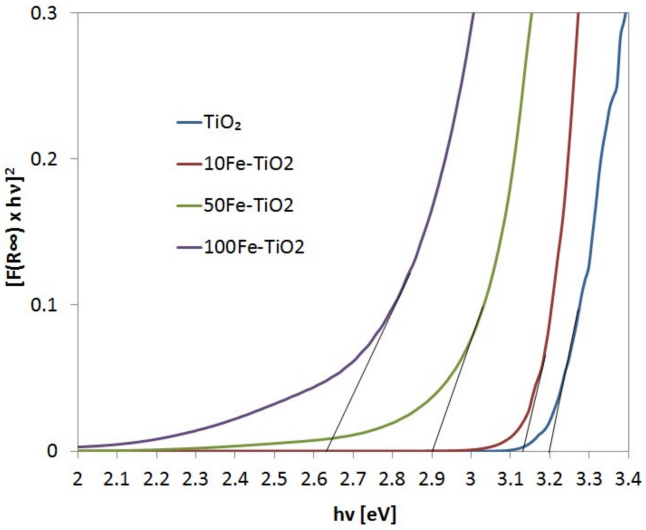

Figure 5. Band gap evaluation of for undoped and Fe-doped TiO_2 photocatalysts.

2.2. Catalyst Screening and Selection

Preliminary experiments were performed to evaluate whether RV5 could be degraded by a photocatalytic treatment. In these experiments, the concentrations of the dye and the catalyst were held constant at 30 ppm and 3 g/L, respectively, so as to operate with a dye-to-catalyst weight ratio of 1:100. The photodegradation process was carried out at the spontaneous pH of the dye solution (pH 7.2) for an overall duration of 10 h (1 h of darkness and 9 h of irradiation). The following catalysts were tested: P-25 Degussa (P-25) and Fe-doped TiO_2 at three Fe levels: 10Fe-TiO_2, 50Fe-TiO_2, and 100Fe-TiO_2. The results are shown in Figure 6.

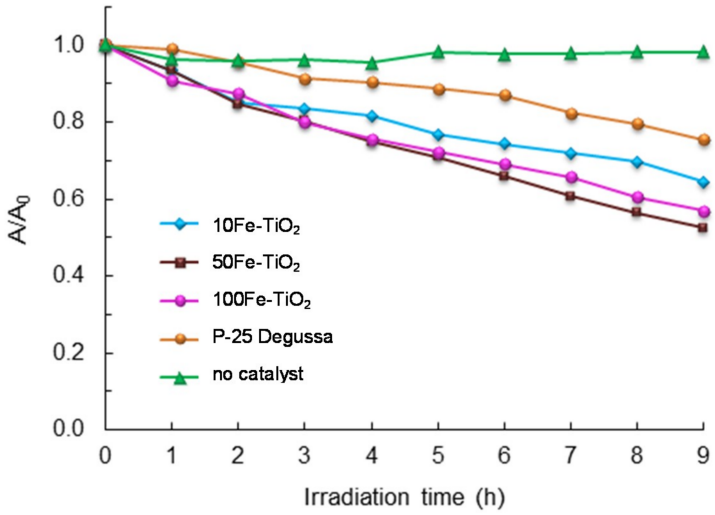

Figure 6. Photocatalytic degradation of Reactive Violet 5 (RV5) in the absence and presence of different catalysts (c^0_{RV5} = 30 ppm; pH = 7.2; catalyst load = 3 g/L). A is the absorbance of the dye solution at 560 nm.

The first point to note is that, in the absence of a catalyst, no significant variations in dye concentration were observed, while all catalysts were able to degrade RV5. The removal efficiencies at the end of the treatment ranged from about 23% (P-25) to 47.6% (50Fe-TiO_2). Furthermore, a closer analysis of the results in Figure 5 reveals that:

- P-25 resulted in a color removal close to 23% at the end of the treatment;
- 100Fe-TiO_2 showed a final decolorization degree close to 42%;
- 10Fe-TiO_2 exhibited an intermediate behavior and decolorized the dye solution to about 35%;
- 50Fe-TiO_2 was the most effective catalyst, with a color removal efficiency of 47.6%.

It is worthwhile to note that, at fixed irradiation time, the degradation performance of 50Fe-TiO_2 was higher than that of the 10Fe-TiO_2 sample. The enhancement in the photocatalytic activity of 50Fe-TiO_2 could have been due to the fact that the Fe^{3+} species could trap the photoexcited electrons and then transfer them to the oxygen molecules, facilitating the electron-hole charge separation and hence suppressing the recombination of the photogenerated electron and hole [43].

It is also interesting to consider that, although the band-gap energy of 100Fe-TiO_2 was smaller than that of 50Fe-TiO_2 (2.63 and 2.90 eV, respectively), the first catalyst exhibited a lower photocatalytic activity. This could have been due to the higher content of Fe(III) ions, which acted as recombination centers for the photogenerated hole-electron pairs [44,45].

Since 50Fe-TiO_2 was the most effective of the catalysts tested, it was selected as the best catalyst for RV5 degradation under visible light irradiation.

2.3. Analysis of the UV–Vis Absorption Spectrum of RV5 During Degradation

Figure 7 shows the UV–Vis spectrum of RV5 and its changes during the photodegradation process. A prominent feature of the dye spectrum was the presence of two main bands centered around 220 and 560 nm. The broad band at 560 nm arose from the chromophoric group of the dye molecule, while the band at 320 nm was related to the aromatic groups in the molecule [46].

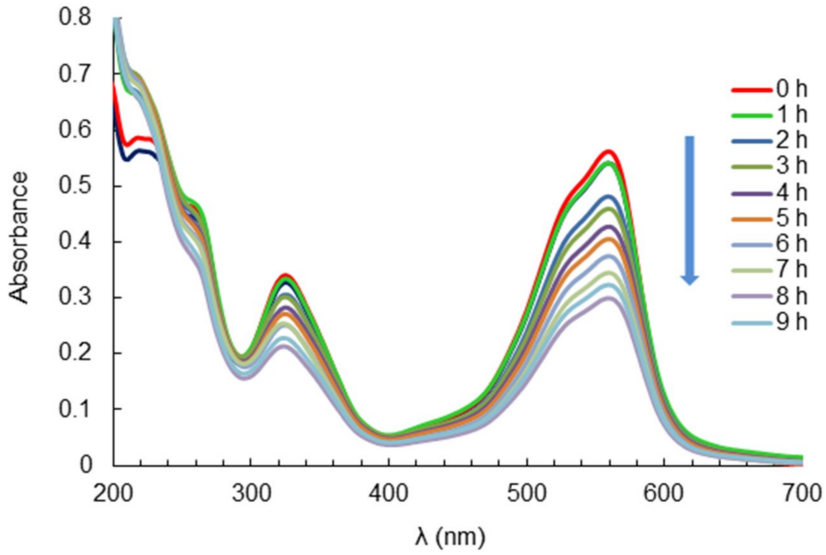

Figure 7. Absorption spectrum of Reactive Violet 5 (RV5) during the photocatalytic treatment.

During photodegradation, the intensity of both bands decreased. The reduction in the intensity of the band at 560 nm indicated a decrease in the conjugation of the chromophore moiety, resulting in a progressive decolorization of the dye solution. The decrease of the band at 220 nm and the spectral changes at lower wavelengths suggested that the aromatic part of the molecule was also affected by the treatment.

Therefore, it can be concluded that the photocatalytic treatment of RV5 by the 50Fe-TiO_2 catalyst was effective not only for color removal, but also for the degradation of the aromatic structures of the dye molecule and its cleavage into smaller fragments.

2.4. Effect of pH

As it is known, pH is one of the most important process parameters for the photocatalytic degradation of dyes. Its role in photocatalytic reactions has been thoroughly investigated and discussed. Evidence from previous studies indicated that pH can affect the photocatalytic degradation of dyes in multiple ways, as it may influence the surface properties of the catalyst, the charge distribution on the dye molecule, and the generation of reactive radical species [47,48]. The overall effect is dependent on the reaction conditions but also on the dye type. This may lead to apparently conflicting results. For example, the highest efficiency for the photocatalytic degradation of azo dye Amido Black 10B was observed at pH 9 [49], while Acid Orange 7 [50] and Acid Yellow 17 [51] showed maximum degradation at pH 3.

In order to find the optimal pH for RV5 degradation, this parameter was varied from 4 to 12. The initial dye concentration was set at 30 ppm and the catalyst load was 3 g/L. The results obtained during a 10 h treatment period (1 h of darkness and 9 h of irradiation) are shown in Figure 8. It can be seen that at lower pH values ($4 \leq pH \leq 8$) the absorbance at 560 nm remained almost constant. By contrast, at pH 10 it decreased quickly, reaching a value close to zero after 2 h of irradiation. At pH 12, an intermediate behavior was observed, with the initial absorbance being halved in about 6 h and reduced by around 80% at the end of the treatment. Thus, it can be concluded that, under the experimental conditions employed, the optimal pH for RV5 degradation was equal to 10. Accordingly, further experiments were carried out at this pH.

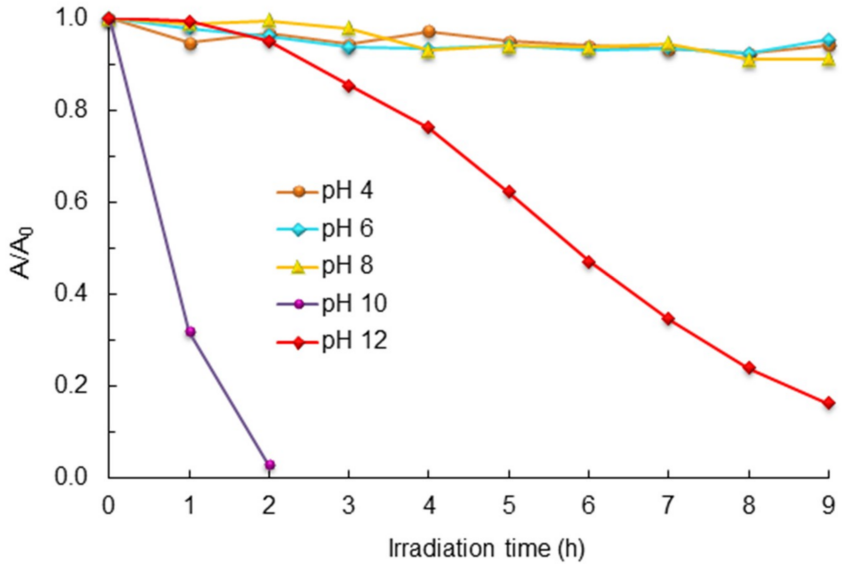

Figure 8. Photocatalytic degradation of Reactive Violet 5 (RV5) at different pH values (c^0_{RV5} = 30 ppm; catalyst load = 3 g/L). A is the absorbance of the dye solution at 560 nm.

The influence of pH on dye removal can be attributed to its effects on the generation of radical species, particularly hydroxyl radicals ($^{\bullet}OH$), during the photocatalytic process. These radicals are produced at the catalyst surface from the oxidation of OH^- or H_2O by the photogenerated holes (h^+):

$$OH^- + h^+ \rightarrow {}^{\bullet}OH, \quad (1)$$

$$H_2O + h^+ \rightarrow {}^{\bullet}OH + H^+. \quad (2)$$

Hydroxyl radicals are powerful oxidizing agents and can easily attack the azo groups in the dye molecule, breaking the –N=N– bonds and causing decolorization of the dye solution. They can also attack the aromatic structures of the dye, but these structures are more resistant than azo bonds, so decolorization is achieved more easily than degradation [52].

From Equation (1) and Equation (2), it can be seen that the production of •OH is favored under alkaline conditions, which is consistent with the results in Figure 8. The enhanced removal of azo dyes at alkaline pH was observed in several other studies. For example, after 40 min of the photocatalytic treatment with TiO_2 of a solution containing Reactive Orange 4, the color removal was 25.3% at pH 1 and 90.5% at pH 9 [53]. The degradation of the dye was less effective, as after 80 min of irradiation, it passed from 15.2% at pH 1 to 87.2% at pH 9. Similar results were obtained in a study on the photocatalytic degradation of Reactive Black 5 by TiO_2 [54].

In addition to the direct effect of pH on the production of •OH, as described by Equation (1) and Equation (2), it should also be considered that [48,55]: (a) The extent of dye adsorption and photon absorption are also affected by pH; (b) at low pH, H^+ ions can interact with the azo bonds, decreasing their electron density and their susceptibility to electrophilic attack by hydroxyl radicals; and (c) under acidic conditions, TiO_2 particles tend to agglomerate, reducing the surface area of the catalyst.

The observed decrease in color removal at pH 12 could be due to a decreased adsorption of dye molecules on the catalyst surface. In fact, at this pH, the catalyst surface is highly hydroxylated and hence negatively charged, repelling the RV5 molecules that have charges of the same sign.

2.5. Effect of Catalyst Load

The amount of catalyst used in the photocatalytic treatment is another important factor for the degradation of pollutants [48]. To evaluate the optimal catalyst load, this quantity was varied from 0 to 6 g/L, keeping the pH at 10 and the initial dye concentration at 30 ppm. The results of these experiments are shown in Figure 9. In the absence of a catalyst, the decolorization of the dye solution proceeded quite slowly, with over 20% of the initial amount of RV5 still present at the end of the treatment. When the catalyst was added at 0.5 g/L, the decolorization was more rapid and was completed in about 4 h. With a catalyst load of 1.5 g/L, this time was reduced to about 3 h. At higher catalyst loads (3 to 6 g/L), about 2 h were sufficient to achieve complete color removal. Furthermore, the observed decay curves were very similar to each other.

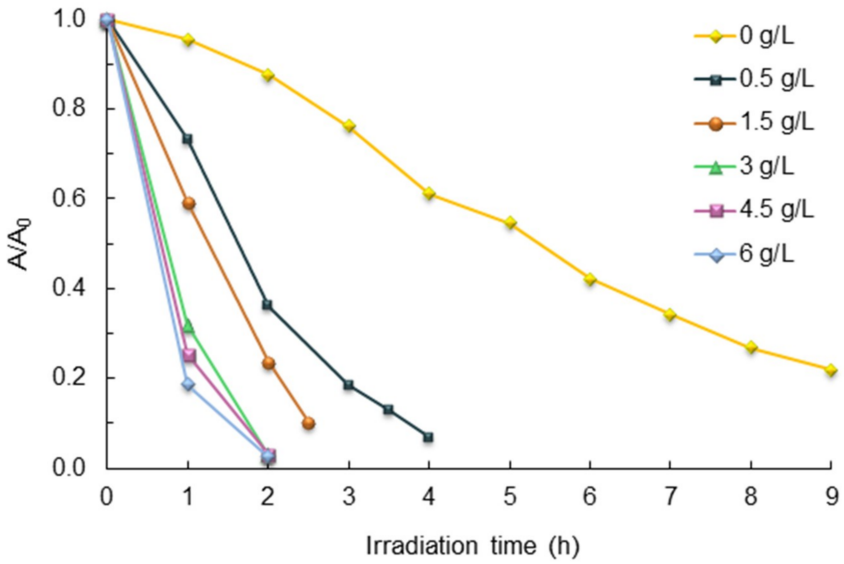

Figure 9. Photocatalytic degradation of Reactive Violet 5 (RV5) at different catalyst loads (c^0_{RV5} = 30 ppm; pH = 10). A is the absorbance the dye solution at 560 nm.

A simple kinetic analysis was used to provide a quantitative description of the effect of catalyst load on dye removal. In particular, the apparent rates of the photocatalytic process were determined by applying the initial rate method.

The initial rate of dye removal ($-r_0$), which is rigorously defined as:

$$-r_0 = -\left.\frac{d(A/A_0)}{dt}\right|_{t=0}, \quad (3)$$

was calculated as:

$$-r_0 = -\frac{(A/A_0)_{t_1} - (A/A_0)_{t_0}}{t_1 - t_0}, \quad (4)$$

with $t_0 = 0$ and $t_1 = 1$ h. In the above equations, A_0 is the absorbance of the dye solution at 560 nm and at the beginning of irradiation ($t = 0$), while A is the absorbance at time t.

From the results in Figure 10 it can be seen that, at catalyst loads lower than 3 g/L, there was a nearly linear increase of the decolorization rate with the amount of catalyst, while the effect was very small above this value. Accordingly, a value of 3 g/L was selected as the optimal catalyst load.

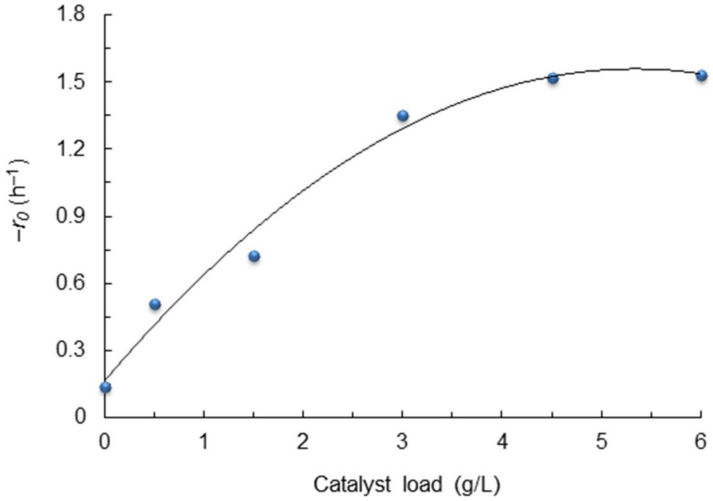

Figure 10. Initial rate of Reactive Violet 5 (RV5) removal as a function of catalyst load (c^0_{RV5} = 30 ppm; pH = 10).

The existence of a threshold value for catalyst load was reported in many studies on the photocatalytic degradation of azo dyes including, for example, Reactive Black 5 [54], Reactive Blue 4 [56], Reactive Orange 4 [57], Reactive Red 120 [58], Reactive Blue 19 [59], Reactive Blue 198, and Reactive Yellow 145 [60]. This behavior is likely the result of multiple factors [46]. At low loadings, an increase in the amount of catalyst in the reaction mixture has a positive effect on the kinetics of dye removal due to the increased surface area available for dye adsorption and degradation. However, when all dye molecules are adsorbed on the catalyst surface, further additions of catalyst are no longer effective for decolorization of the dye solution. Moreover, an excessive amount of catalyst can reduce light penetration in the solution due to shielding and scattering effects resulting from aggregate formation. Finally, activated catalyst particles can interact with ground-state particles causing partial deactivation of the catalyst.

2.6. Effect of Hydrogen Peroxide

Hydrogen peroxide is a strong oxidizing agent and is widely used in several AOPs for the degradation of pollutants in combination with ozone, UV, ultrasounds, microwaves, and other agents [61,62]. Furthermore, it can also be added to the reaction medium during photocatalytic treatment to improve the efficiency of the process through the production of additional radical species. For example, Domingues et al. [63] investigated the hydrogen peroxide-assisted photocatalytic degradation of a dyeing factory effluent using TiO_2 or ZnO as catalysts. The authors found that the addition of hydrogen peroxide at a concentration of 10^{-2} M to the effluent significantly increased

the removal of dyes without generating secondary pollutants. Similarly, a remarkable increase in the degradation of a textile wastewater, Ce-doped titania, was observed in the presence of hydrogen peroxide at concentrations of up to 2×10^{-2} M [64]. Tian et al. [65] showed that hydrogen peroxide at 50 mM synergistically enhanced the degradation of phenol by precious metal-supported titania catalysts. In another study on the photocatalytic degradation of monochlorobenzene (MCB) in TiO_2 aqueous suspensions [66], the presence of hydrogen peroxide was found to significantly improve treatment efficiency. In particular, the optimal H_2O_2 dosages for MCB degradation and mineralization were, equal to 22.5 and 45 mg L^{-1}, respectively.

To investigate the effect of hydrogen peroxide on the decolorization of RV5, experiments were performed by adding 10 to 100 mM hydrogen peroxide to a solution at pH 10 containing 30 ppm of dye and 3 g/L of catalyst. The results are presented in Figure 11. As can be seen, the color removal efficiency increased upon addition of hydrogen peroxide, but the observed decolorization profiles varied non-monotonically with the amount of hydrogen peroxide present in the reaction medium. This can be better appreciated in Figure 12, where the initial rate of dye removal, calculated from Equation (4), was plotted against the initial hydrogen peroxide concentration. These data revealed that an optimal hydrogen peroxide concentration of 60 mM exists. Similar results were found in other studies on the photocatalytic decolorization of azo dyes under visible light irradiation [54,57,59,67,68].

Since the photodegradation experiments were performed under vigorous agitation using finely powdered catalyst particles, the process can be assumed to be under kinetic control. Accordingly, the observed behavior can be interpreted as the result of the reactions taking place in the system. In particular, it should be considered that hydrogen peroxide, as an electron acceptor, can produce hydroxyl radicals through the following reaction:

$$H_2O_2 + e^- \rightarrow {}^{\bullet}OH + OH^-. \quad (5)$$

Additional hydroxyl radicals can be formed from the reaction of hydrogen peroxide with the superoxide radical:

$$H_2O_2 + O_2^- \rightarrow O_2 + {}^{\bullet}OH + OH^-. \quad (6)$$

However, at high concentrations, hydrogen peroxide can act as a scavenger of hydroxyl radicals, according to the following reactions [55]:

$$H_2O_2 + {}^{\bullet}OH \rightarrow HO_2{}^{\bullet} + H_2O, \quad (7)$$

$$HO_2{}^{\bullet} + {}^{\bullet}OH \rightarrow H_2O + O_2, \quad (8)$$

$$2\,HO_2{}^{\bullet} \rightarrow H_2O_2 + O_2. \quad (9)$$

Furthermore, it can also react with TiO_2 to form peroxy compounds that are detrimental to the degradation process [69]. When the positive and negative effects balance each other, an optimum [70] is found for the amount of hydrogen peroxide in the reaction medium.

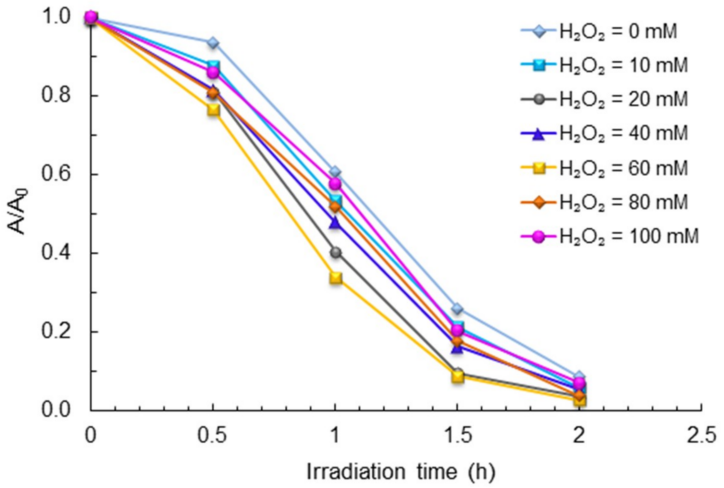

Figure 11. Photocatalytic degradation of Reactive Violet 5 (RV5) at different hydrogen peroxide concentrations (c^0_{RV5} = 30 ppm; pH = 10; catalyst load = 3 g/L). A is the absorbance the dye solution at 560 nm.

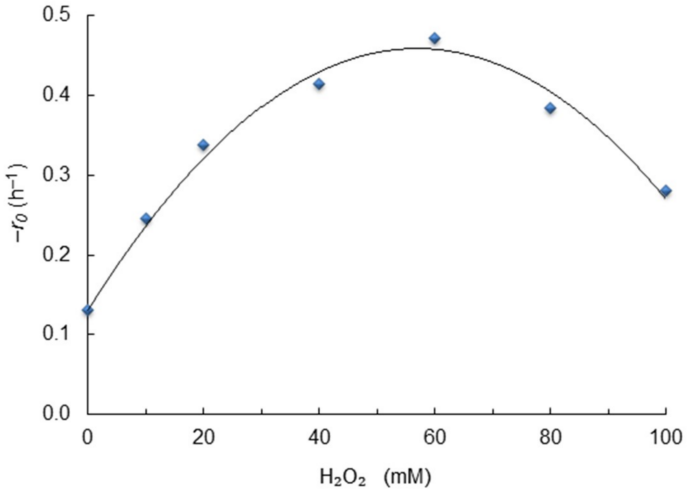

Figure 12. Initial rate of Reactive Violet 5 (RV5) removal as a function of hydrogen peroxide concentration (c^0_{RV5} = 30 ppm; pH = 10; catalyst load = 3 g/L).

2.7. Comparison with the Results of Other Published Studies

It may be interesting to compare the present results with those obtained in other studies on the degradation of RV5.

Chung and Chen [27] investigated the photocatalytic degradation of RV5 using TiO_2 nanoparticles under UV irradiation. Under optimized conditions, the photodegradation efficiency was 90% after 20 min of irradiation and reached nearly 100% after 80 min.

Cabansag et al. [28] studied the degradation of RV5 under UV light with bulk zinc oxide slurry as the photocatalyst. Under optimized conditions, the dye was degraded by 74% after 30 min of irradiation and almost completely after 90 min.

Kunal et al. [29] used an acclimatized indigenous bacterial mixed culture isolated from a dye-contaminated soil to degrade RV5. The mixed culture was composed of six bacterial strains, including *Bacillus*, *Lysinibacillus*, and *Ochrobacterium* species, and was grown in a minimal medium containing glucose and yeast extract. Under static growth conditions at 37 °C and pH 7, the dye solution was completely decolorized in about 18 h. However, in the absence of carbon and nitrogen sources, only about 4% of the initial amount of dye was degraded after the same amount of time, indicating that these sources are essential for the treatment.

Bheemaraddi et al. [30] investigated the ability of a bacterial strain of *Paracoccus* sp. isolated from a textile mill effluent to degrade RV5 as the sole source of carbon. Under static conditions and with minimal nutritional requirements this strain allowed complete decolorization of the dye solution within 16 h.

Finally, Ayed et al. [31] explored the feasibility of using a consortium of *Staphylococcus* species, two of which were isolated from a textile wastewater, to degrade RV5. Under optimal conditions, the dye solution was completely (>99%) decolorized within 8 h. The decolorization was also accompanied by a high COD (Chemical Oxygen Demand) removal (94.93%)

Therefore, the results obtained in the present study indicate that the degradation of RV5 by a Fe-doped titania catalyst under visible light irradiation can lead to dye removal efficiencies that are comparable with those reported for UV-photocatalytic or microbial treatments. Moreover, compared to microbial degradation processes, the investigated technology is simpler to implement and more flexible in operation.

3. Materials and Methods

3.1. Materials

Sodium hydroxide (NaOH, CAS 1310-73-2), sodium hydrogen carbonate ($NaHCO_3$, CAS 144-55-8), disodium hydrogen phosphate (Na_2HPO_4, CAS 7558-79-4), potassium dihydrogen phosphate (KH_2PO_4, CAS 7778-77-0), sodium acetate (CH_3COONa, CAS 127-09-3), acetic acid (CH_3COOH, CAS 64-19-7) and hydrogen peroxide (30 wt% in water, CAS 7722-84-1), iron acetylacetonate ($Fe(C_5H_7O_2)_3$, CAS 14024-18-1), and titanium isopropoxide ($C_{12}H_{28}O_4Ti$, CAS 546-68-9) were purchased from Sigma-Aldrich Co. (St. Louis, Mo, USA). All chemicals were reagent grade and used as received.

RV5 of technical grade ($C_{20}H_{16}N_3Na_3O_{15}S_4$, MW 735.59 g mol^{-1}, color index number 18097) was provided by Gammacolor Srl (Seveso, Italy) and used as received. The natural pH of the dye solution was 7.2 ± 0.1. When needed, RV5 was dissolved in the following buffers: Acetate buffer (0.1 M, pH 4), phosphate buffer (0.1 M, pH 6 and 8). and carbonate buffer (0.1 M, pH 10 and 12).

3.2. Catalyst Preparation and Characterization

P-25 Degussa was obtained from Sigma-Aldrich Co. (St. Louis, Mo, USA). Fe-TiO_2 photocatalysts were prepared by the sol-gel method. In particular, 50 mg of iron acetylacetonate was dissolved in 25 mL of titanium isopropoxide. The obtained solution was sonicated in order to obtain the complete solubilization of iron acetylacetonate. Then, 100 mL of distilled water were added to obtain a precipitate which was separated from the liquid phase by centrifugation for 5 min at 5000 rpm. The sample was washed with distilled water for three times to remove any impurities and then calcined at 450 °C for 30 min [26]. The obtained samples were named xFe-TiO_2, where x is the amount (in mg) of iron acetylacetonate used in the synthesis. The list of the prepared photocatalysts with the amount of chemicals used in the preparation procedure is reported in Table 2.

Table 2. List of the prepared photocatalysts, amount of chemicals used in the synthesis, and Fe/Ti molar ratio.

Photocatalysts	$Fe(C_5H_7O_2)_3$ Amount [mg]	Titanium Isopropoxide [mL]	Distilled Water [mL]	Fe/Ti Molar Ratio [mol/mol]
TiO_2	0	25	100	0
10Fe-TiO_2	10	25	100	0.00033
50Fe-TiO_2	50	25	100	0.0017
100Fe-TiO_2	100	25	100	0.0033

All of the photocatalysts were characterized using different techniques. The Raman spectra of the samples were recorded with a Dispersive MicroRaman system (Renishaw InVia, Wotton-under-Edge,

Gloucestershire, UK), equipped with a 514 nm laser, in the range of 100–2000 cm^{-1} Raman shift. The crystal phases of photocatalysts were determined by XRD analysis, which was carried out on Bruker D8 diffractometer (Bruker Corporation, Madison, WI, USA) using Cu-Kα radiation. The surface area (SSA) of the catalysts was obtained from the dynamic N_2 adsorption measurement at −196 °C, using a Costech Sorptometer 1042 instrument (Costech International, Milano, Italy), after a pre-treatment of the samples at 150 °C for 30 min in He flow. UV–vis reflectance spectra of powder catalysts were recorded by a Perkin Elmer spectrometer Lambda 35 using an RSA-PE-20 reflectance spectroscopy accessory (Labsphere Inc., North Sutton, NH, USA). All spectra were obtained using an 8° sample positioning holder, giving total reflectance relative to a calibrated standard SRS-010-99 (Labsphere Inc., North Sutton, NH, USA). Equivalent band gap determinations of the photocatalysts were obtained using the Kubelka–Munk function $F(R_\infty)$ by plotting $[F(R_\infty) \times h\nu]^2$ vs. $h\nu$.

3.3. Photocatalytic Apparatus

The experimental apparatus consisted of a borosilicate glass cylindrical photoreactor (ID = 3 cm, H = 18 cm) equipped with an air distributor and a magnetic bar. A commercial flexible light-emitting diode (LED) strip (SMD 5050, 60 LED/m, 0.24 W/LED), with an overall length of 1.5 m, was wrapped around the reactor and used as light source. The LEDs emitted in the wavelength range of 460–470 nm, with a maximum emission at 465 nm. The air distributor provided a maximum flow rate of 300 NL/h and was placed at the bottom of the reactor, just above the stirring bar. Darkness conditions were achieved by covering the photocatalytic apparatus with an aluminum foil.

3.4. Photodegradation Experiments

Photodegradation experiments were carried out by putting 50 mL of the aqueous solution containing the dye and the catalyst in the reactor. The system was left in the dark under stirring for 1 h to allow the adsorption–desorption equilibrium of RV5 on the photocatalyst surface. Then, the light source was switched on and the reactor was aerated. At the desired time, a small sample of liquid was taken, filtered at 0.45 μm, and analyzed spectrophotometrically. Measurements were made on a double-beam UV–vis spectrophotometer (UV-2700, Shimadzu, Kyoto, Japan) at 560 nm, where the absorption spectrum of RV5 displayed a maximum. The stirring rate was set at 400 rpm and the air flow rate at 200 NL/h. These values were selected from the results of preliminary experiments (data not shown) aimed at evaluating the influence of the external mass transfer resistance on the photodegradation kinetics. In these experiments, the stirring rate was increased up to 600 rpm and the air flow rate up to 400 NL/h, while keeping all other parameters constant, in order to identify the conditions under which the external mass transfer resistance could be considered negligible.

The initial dye concentration was varied between 20 and 100 ppm and the catalyst load between 0.5 and 6 g/L. In experiments with hydrogen peroxide, this component was added at a final concentration of 10 to 100 mM in the reaction medium.

4. Conclusions

The presence of dyes in industrial effluents is an issue of major concern due to the detrimental effects that these pollutants may have on the environment. In this study, we have shown that RV5, an azo dye widely used in the textile industry, can be effectively degraded by a photocatalytic treatment using a Fe-doped TiO_2 catalyst under visible light irradiation. An analysis of the effects on the dye removal efficiency of the main process parameters (pH, catalyst load, and hydrogen peroxide concentration) showed that the treatment can be optimized to provide rapid and complete degradation. The use of visible light and the relatively short treatment times make the proposed process a promising and cost-effective method for the removal of dyes from textile effluents.

Future studies should be directed at investigating the effects of the treatment on dye mineralization and evaluating the optimal conditions for mineralization. The identification of the reaction products and

intermediates formed during the photocatalytic process could be helpful to elucidate the mechanisms involved in RV5 degradation.

Author Contributions: Methodology, A.Z., R.L., V.V., and G.I.; investigation, M.M.M.; writing—original draft preparation, A.Z. and G.I.; writing—review and editing, R.L. and V.V.

Funding: This research was partially supported by grants from Sapienza University of Rome (Italy).

Conflicts of Interest: The authors declare no conflict of interest.

References

1. Hunger, K. *Industrial Dyes: Chemistry, Properties, Applications*; Wiley-VCH: Weinheim, Germany, 2003.
2. Clark, M. *Handbook of Textile and Industrial Dyeing – Volume 1: Principles, Processes and Types of Dyes*; Woodhead Publishing: Cambridge, UK, 2011; pp. 428–438.
3. Zuorro, A.; Maffei, G.; Lavecchia, R. Kinetic modeling of azo dye adsorption on non-living cells of *Nannochloropsis* oceanica. *J. Environ. Chem. Eng.* **2017**, *5*, 4121–4127. [CrossRef]
4. Petrucci, E.; Di Palma, L.; Lavecchia, R.; Zuorro, A. Treatment of diazo dye Reactive Green 19 by anodic oxidation on a boron-doped diamond electrode. *J. Ind. Eng. Chem.* **2015**, *26*, 116–121. [CrossRef]
5. Yaseen, D.A.; Scholz, M. Textile dye wastewater characteristics and constituents of synthetic effluents: A critical review. *Int. J. Environ. Sci. Technol.* **2019**, *16*, 1193–1226. [CrossRef]
6. Ventura-Camargo, B.C.; Marin-Morales, M.A. Azo dyes: Characterization and toxicity—A review. *Text. Light Ind. Sci. Technol.* **2013**, *2*, 85–103.
7. Chung, K.-T. Azo dyes and human health: A review. *J. Environ. Sci. Health Pt. C-Environ. Carcinog. Ecotoxicol. Rev.* **2016**, *34*, 233–261. [CrossRef]
8. Parvathi, C.; Maruthavanan, T.; Sivamani, S.; Prakash, C. Removal of dyes from textile wet processing industry: A review. *J. Text. Assoc.* **2011**, *71*, 319–323.
9. Singh, K.; Arora, S. Removal of synthetic textile dyes from wastewaters: A critical review on present treatment technologies. *Crit. Rev. Environ. Sci. Technol.* **2011**, *41*, 807–878. [CrossRef]
10. Vogelpohl, A.; Kim, S.M. Advanced oxidation processes AOPs in wastewater treatment. *J. Ind. Eng. Chem.* **2004**, *10*, 33–40.
11. Oturan, M.A.; Aaron, J.-J. Advanced oxidation processes in water/wastewater treatment: Principles and applications. A review. *Crit. Rev. Environ. Sci. Technol.* **2014**, *44*, 2577–2641. [CrossRef]
12. Kanan, S.; Moyet, M.A.; Arthur, R.B.; Patterson, H.H. Recent advances on TiO_2-based photocatalysts toward the degradation of pesticides and major organic pollutants from water bodies. *Catal. Rev.-Sci. Eng.* **2019**. [CrossRef]
13. Wankhade Atul, V.; Gaikwad, G.S.; Dhonde, M.G.; Khaty, N.T.; Thakare, S.R. Removal of organic pollutant from water by heterogenous photocatalysis: A review. *Res. J. Chem. Environ.* **2013**, *17*, 84–94.
14. Huang, D.-G.; Liao, S.-J.; Liu, J.-M.; Dang, Z.; Petrik, L. Preparation of visible-light responsive N-F-codoped TiO2 photocatalyst by a sol-gel-solvothermal method. *J. Photochem. Photobiol. A-Chem.* **2006**, *184*, 282–288. [CrossRef]
15. Whang, T.J.; Huang, H.Y.; Hsieh, M.T.; Chen, J.J. Laser-induced silver nanoparticles on titanium oxide for photocatalytic degradation of methylene blue. *Int. J. Mol. Sci.* **2009**, *10*, 4707–4718. [CrossRef] [PubMed]
16. Yang, X.; Ma, F.; Li, K.; Guo, Y.; Hu, J.; Li, W.; Huo, M.; Guo, Y. Mixed phase titania nanocomposite codoped with metallic silver and vanadium oxide: New efficient photocatalyst for dye degradation. *J. Hazard. Mater.* **2009**, *175*, 429–438. [CrossRef]
17. Chen, F.; Zou, W.; Qu, W.; Zhang, J. Photocatalytic performance of a visible light TiO_2 photocatalyst prepared by a surface chemical modification process. *Catal. Commun.* **2009**, *10*, 1510–1513. [CrossRef]
18. Huang, M.; Xu, C.; Wu, Z.; Huang, Y.; Lin, J.; Wu, J. Photocatalytic discolorization of methyl orange solution by Pt modified TiO_2 loaded on natural zeolite. *Dyes Pigment.* **2008**, *77*, 327–334. [CrossRef]
19. Kumar, S.G.; Devi, L.G. Review on modified TiO_2 photocatalysis under UV/visible light: Selected results and related mechanisms on interfacial charge carrier transfer dynamics. *J. Phys. Chem. A* **2011**, *115*, 13211–13241. [CrossRef] [PubMed]
20. Lee, H.; Shin, M.; Lee, M.; Hwang, Y.J. Photo-oxidation activities on Pd-doped TiO_2 nanoparticles: Critical PdO formation effect. *Appl. Catal. B-Environ.* **2015**, *165*, 20–26. [CrossRef]

21. Abd El-Rady, A.A.; Abd El-Sadek, M.S.; El-Sayed Breky, M.M.; Assaf, F.H. Characterization and photocatalytic efficiency of palladium doped-TiO_2 nanoparticles. *Adv. Nanopart.* **2013**, *2*, 372–377. [CrossRef]
22. Sood, S.; Umar, A.; Mehta, S.K.; Kansal, S.K. Highly effective Fe-doped TiO_2 nanoparticles photocatalysts for visible-light driven photocatalytic degradation of toxic organic compounds. *J. Colloid Interface Sci.* **2015**, *450*, 213–223. [CrossRef]
23. Mathew, S.; Ganguly, P.; Rhatigan, S.; Kumaravel, V.; Byrne, C.; Hinder, S.; Bartlett, J.; Nolan, M.; Pillai, S.C. Cu doped TiO_2: Visible light assisted photocatalytic antimicrobial activity and high temperature anatase stability. *ChemRxiv* **2018**. [CrossRef]
24. Moradi, V.; Jun, M.B.G.; Blackburn, A.; Herring, R.A. Significant improvement in visible light photocatalytic activity of Fe doped TiO_2 using an acid treatment process. *Appl. Surf. Sci.* **2018**, *427*, 791–799. [CrossRef]
25. Su, R.; Bechstein, R.; Kibsgaard, J.; Vang, R.T.; Besenbacher, F. High-quality Fe-doped TiO_2 films with superior visible-light performance. *J. Mat. Chem.* **2012**, *22*, 23755–23758. [CrossRef]
26. Iervolino, G.; Vaiano, V.; Rizzo, L. Visible light active Fe-doped TiO_2 for the oxidation of arsenite to arsenate in drinking water. *Chem. Eng. Trans.* **2018**, *70*, 1573–1578.
27. Chung, Y.C.; Chen, C.Y. Degradation of azo dye reactive violet 5 by TiO_2 photocatalysis. *Environ. Chem. Lett.* **2009**, *7*, 347–352. [CrossRef]
28. Cabansag, J.L.J.; Dumelod, J.C.; Alfaro, J.C.O.; Arsenal, J.D.; Sambot, J.C.; Enerva, L.T.; Leaño, J.L., Jr. Photocatalytic degradation of aqueous C.I. Reactive Violet 5 using bulk zinc oxide (ZnO) slurry. *Philipp. J. Sci.* **2013**, *142*, 77–85.
29. Kunal, J.; Varun, S.; Digantkumar, C.; Datta, M. Decolorization and degradation of azo dye—Reactive Violet 5R by an acclimatized indigenous bacterial mixed cultures-SB4 isolated from anthropogenic dye contaminated soil. *J. Hazard. Mat.* **2012**, *213–214*, 378–386.
30. Bheemaraddi, M.C.; Patil, S.; Shivannavar, C.T.; Gaddad, S.M. Isolation and characterization of *Paracoccus* sp. GSM2 capable of degrading textile azo dye Reactive Violet 5. *Sci. World J.* **2014**, *2014*, 410704. [CrossRef]
31. Ayed, L.; Bekir, K.; Achour, S.; Cheref, A.; Bakhrouf, A. Exploring bioaugmentation strategies for azo dye CI Reactive Violet 5 decolourization using bacterial mixture: Dye response surface methodology. *Water Environ. J.* **2017**, *31*, 80–89. [CrossRef]
32. Fidaleo, M.; Lavecchia, R.; Petrucci, E.; Zuorro, A. Application of a novel definitive screening design to decolorization of an azo dye on boron-doped diamond electrodes. *Int. J. Environ. Sci. Technol.* **2016**, *13*, 835–842. [CrossRef]
33. Vaiano, V.; Iervolino, G.; Sannino, D.; Rizzo, L.; Sarno, G. MoOx/TiO_2 immobilized on quartz support as structured catalyst for the photocatalytic oxidation of As(III) to As(V) in aqueous solutions. *Chem. Eng. Res. Des.* **2016**, *109*, 190–199. [CrossRef]
34. Pongwan, P.; Inceesungvorn, B.; Wetchakun, K.; Phanichphant, S.; Wetchakun, N. Highly efficient visible-light-induced photocatalytic activity of Fe-doped TiO_2 nanoparticles. *Eng. J.* **2012**, *16*, 143–151. [CrossRef]
35. Li, Z.; Shen, W.; He, W.; Zu, X. Effect of Fe-doped TiO_2 nanoparticle derived from modified hydrothermal process on the photocatalytic degradation performance on methylene blue. *J. Hazard. Mater.* **2008**, *155*, 590–594. [CrossRef] [PubMed]
36. Sun, L.; Zhai, J.; Li, H.; Zhao, Y.; Yang, H.; Yu, H. Study of homologous elements: Fe, Co, and Ni dopant effects on the photoreactivity of TiO_2 nanosheets. *ChemCatChem* **2014**, *6*, 339–347. [CrossRef]
37. Yang, Y.; Yu, Y.; Wang, J.; Zheng, W.; Cao, Y. Doping and transformation mechanisms of Fe^{3+} ions in Fe-doped TiO_2. *CrystEngComm* **2017**, *19*, 1100–1105. [CrossRef]
38. Marami, M.B.; Farahmandjou, M.; Khoshnevisan, B. Sol–gel synthesis of Fe-doped TiO_2 nanocrystals. *J. Electron. Mater.* **2018**, *47*, 3741–3748. [CrossRef]
39. Zhou, M.; Yu, J.; Cheng, B. Effects of Fe-doping on the photocatalytic activity of mesoporous TiO_2 powders prepared by an ultrasonic method. *J. Hazard. Mater.* **2006**, *137*, 1838–1847. [CrossRef] [PubMed]
40. Gao, Y.; Luan, T.; LÜ, T.; Cheng, K.; Xu, H. Performance of V_2O_5-WO_3-MoO_3/TiO_2 catalyst for selective catalytic reduction of NO_x by NH_3. *Chin. J. Chem. Eng.* **2013**, *21*, 1–7. [CrossRef]
41. Prajapati, B.; Kumar, S.; Kumar, M.; Chatterjee, S.; Ghosh, A.K. Investigation of the physical properties of Fe:TiO_2-diluted magnetic semiconductor nanoparticles. *J. Mater. Chem. C* **2017**, *5*, 425–4267. [CrossRef]

42. Wang, W.; Tadé, M.O.; Shao, Z. Research progress of perovskite materials in photocatalysis and photovoltaics-related energy conversion and environmental treatment. *Chem. Soc. Rev.* **2015**, *44*, 5371–5408. [CrossRef]
43. Ali, T.; Tripathi, P.; Azam, A.; Raza, W.; Ahmed, A.S.; Ahmed, A.; Muneer, M. Photocatalytic performance of Fe-doped TiO_2 nanoparticles under visible-light irradiation. *Mater. Res. Express* **2017**, *4*, aa576d. [CrossRef]
44. Navio, J.A.; Testa, J.J.; Djedjeian, P.; Padron, J.R.; Rodriguez, D. Iron-doped titania powders prepared by a sol–gel method. Part II: Photocatalytic properties. *Appl. Catal. A-Gen.* **1999**, *178*, 191–203. [CrossRef]
45. Serpone, N.; Lawless, D.; Disdier, D. Spectroscopic, photoconductivity, and photocatalytic studies of TiO_2 colloids: Naked and with the lattice doped with Cr^{3+}, Fe^{3+}, and V^{5+} cations. *Langmuir* **1994**, *10*, 643–652. [CrossRef]
46. Petrucci, E.; Di Palma, L.; Lavecchia, R.; Zuorro, A. Modeling and optimization of Reactive Green 19 oxidation on a BDD thin-film electrode. *J. Taiwan Inst. Chem. Eng.* **2015**, *51*, 152–158. [CrossRef]
47. Rauf, M.A.; Ashraf, S.S. Fundamental principles and application of heterogeneous photocatalytic degradation of dyes in solution. *Chem. Eng. J.* **2009**, *151*, 10–18. [CrossRef]
48. Ajmal, A.; Majeed, I.; Malik, R.N.; Idriss, H.; Nadeem, M.A. Principles and mechanisms of photocatalytic dye degradation on TiO_2 based photocatalysts: A comparative overview. *RSC Adv.* **2014**, *4*, 37003–37026. [CrossRef]
49. Qamar, M.; Saquib, M.; Muneer, M. Photocatalytic degradation of two selected dye derivatives, chromotrope 2B and amido black 10B, in aqueous suspensions of titanium dioxide. *Dyes Pigment.* **2005**, *65*, 1–9. [CrossRef]
50. Behnajady, M.A.; Modirshahla, N.; Shokri, M. Photodestruction of acid orange 7 (AO7) in aqueous solutions by UV/H_2O_2: Influence of operational parameters. *Chemosphere* **2005**, *55*, 129–134. [CrossRef]
51. Khanna, A.; Shetty K, V. Solar photocatalysis for treatment of Acid Yellow-17 (AY-17) dye contaminated water using Ag@TiO_2 core-shell structured nanoparticles. *Environ. Sci. Pollut. Res.* **2013**, *20*, 5692–5707. [CrossRef]
52. Wu, C.H. Photodegradation of C.I. Reactive Red 2 in UV/TiO_2-based systems: Effects of ultrasound irradiation. *J. Hazard. Mat.* **2009**, *167*, 434–439. [CrossRef]
53. Muruganandham, M.; Swaminathan, M. Solar photocatalytic degradation of a reactive azo dye in TiO_2-suspension. *Sol. Energy Mater. Sol. Cells* **2004**, *81*, 439–457. [CrossRef]
54. Muruganandham, M.; Sobana, N.; Swaminathan, M. Solar assisted photocatalytic and photochemical degradation of Reactive Black 5. *J. Hazard. Mater.* **2006**, *137*, 1371–1376. [CrossRef]
55. Fox, M.A.; Dulay, M.T. Heterogeneous photocatalysis. *Chem. Rev.* **1993**, *93*, 341–357. [CrossRef]
56. Samsudin, E.M.; Goh, S.N.; Wu, T.Y.; Ling, T.T.; Hamid, S.B.A.; Juan, J.C. Evaluation on the photocatalytic degradation activity of Reactive Blue 4 using pure anatase nano-TiO_2. *Sains Malays.* **2015**, *44*, 1011–1019. [CrossRef]
57. Gonçalves, M.S.T.; Pinto, E.M.S.; Nkeonye, P.; Oliveira-Campos, A.M.F. Degradation of C.I. Reactive Orange 4 and its simulated dyebath wastewater by heterogeneous photocatalysis. *Dyes Pigment.* **2005**, *64*, 135–139. [CrossRef]
58. Kavitha, S.K.K.; Palanisamy, P.N. Photocatalytic and sonophotocatalytic degradation of Reactive Red 120 using dye sensitized TiO_2 under visible light. *World Acad. Sci. Eng. Technol.* **2011**, *73*, 1–6.
59. Saquib, M.; Muneer, M. Semiconductor mediated photocatalysed degradation of an anthraquinone dye, Remazol Brilliant Blue R under sunlight and artificial light source. *Dyes Pigment.* **2002**, *53*, 237–249. [CrossRef]
60. Thamaraiselvi, K.; Sivakumar, T. Photocatalytic activities of novel $SrTiO_3$–BiOBr heterojunction catalysts towards the degradation of reactive dyes. *Appl. Catal. B-Environ.* **2017**, *207*, 218–232.
61. Guan, R.; Yuan, X.; Wu, Z.; Liang, L.; Li, Y.; Zeng, G. Principle and application of hydrogen peroxide based advanced oxidation processes in activated sludge treatment: A review. *Chem. Eng. J.* **2018**, *339*, 519–530. [CrossRef]
62. Asghar, A.; Raman, A.A.A.; Daud, W.M.A.W. Advanced oxidation processes for in-situ production of hydrogen peroxide/hydroxyl radical for textile wastewater treatment: A review. *J. Clean. Prod.* **2015**, *87*, 826–838. [CrossRef]
63. Domingues, F.S.; Freitas, T.K.F.D.S.; de Almeida, C.A.; de Souza, R.P.; Ambrosio, E.; Palácio, S.M.; Garcia, J.C. Hydrogen peroxide-assisted photocatalytic degradation of textile wastewater using titanium dioxide and zinc oxide. *Environ. Technol.* **2019**, *40*, 1223–1232. [CrossRef]

64. Touati, A.; Hammedi, T.; Najjar, W.; Ksibi, Z.; Sayadi, S. Photocatalytic degradation of textile wastewater in presence of hydrogen peroxide: Effect of cerium doping titania. *J. Ind. Eng. Chem.* **2016**, *35*, 36–44. [CrossRef]
65. Tseng, D.-H.; Juang, L.-C.; Huang, H.-H. Effect of oxygen and hydrogen peroxide on the photocatalytic degradation of monochlorobenzene in TiO_2 aqueous suspension. *Int. J. Photoenergy* **2012**, *2012*, 328526. [CrossRef]
66. Tian, F.; Zhu, R.; Song, K.; Ouyang, F.; Cao, G. Synergistic photocatalytic degradation of phenol using precious metal supported titanium dioxide with hydrogen peroxide. *Environ. Eng. Sci.* **2016**, *33*, 185–192. [CrossRef]
67. Neppolian, B.; Choi, H.C.; Sakthivel, S.; Arabindoo, B.; Murugesan, V. Solar light induced and TiO_2 assisted degradation of textile dye reactive blue 4. *Chemosphere* **2002**, *46*, 1173–1181. [CrossRef]
68. Thi Dung, N.; Van Khoa, N.; Herrmann, J.M. Photocatalytic degradation of reactive dye RED-3BA in aqueous TiO_2 suspension under UV-visible light. *Int. J. Photoenergy* **2005**, *7*, 11–15. [CrossRef]
69. Poulios, I.; Tsachpinis, I. Photodegradation of the textile dye Reactive Black 5 in the presence of semiconducting oxides. *J. Chem. Technol. Biotechnol.* **1999**, *74*, 349–357. [CrossRef]
70. Zuorro, A.; Maffei, G.; Lavecchia, R. Effect of solvent type and extraction conditions on the recovery of Phenolic compounds from artichoke waste. *Chem. Eng. Trans.* **2014**, *39*, 463–468.